

Ion microprobe analyses of exsolution lamellae in peristerites and cryptoperthites

YASUNORI MIÚRA¹ AND JOHN C. RUCKLIDGE

Department of Geology, University of Toronto
Toronto, Ontario, Canada M5S 1A1

Abstract

Combined data from electron microscope, electron microprobe, and ion microprobe analyzers can be used to determine the composition and thickness of lamellae in peristerite and cryptoperthite feldspars. Blue iridescent peristerite from Hybla, Ontario has a bulk composition of An_5Or_1 and lamellae compositions of An_2Or_1 and $An_{19}Or_1$. Orange-red iridescent peristerite from the same location has a bulk composition of An_7Or_1 , and lamellae of An_2Or_1 and $An_{23}Or_3$. Two pale blue iridescent cryptoperthites from Quebec and Johana, Japan have the following compositions: $An_{11}Or_{30}$ (bulk) and $An_{19}Or_{15}$, An_0Or_{51} for lamellae; An_1Or_{50} (bulk) and An_6Or_{35} , An_0Or_{72} for lamellae. The irregular nature of the lamellae in peristerites and cryptoperthites precludes ion microprobe depth profiling, such as has been applied to more regular labradorite lamellae. Point analysis must be performed instead, which may result in possible overlap onto adjacent lamellae and compositional values that do not reflect the extreme limits.

Introduction

Exsolution lamellae in peristerite and cryptoperthite are usually well under $0.1 \mu m$ in thickness. As this is below the spatial resolution of conventional electron probe microanalysis (EPMA), and the detection of minor contents of alkali ions is not reliable using analytical electron microscopy, the surface analysis and sputtering properties of the ion microprobe analyzer (IMA) can be used to make depth profiles through the lamellae.

Miúra and Tomisaka (1978) reported results of an ion microprobe study of exsolution lamellae in labradorite. They determined the An and Or contents from working curves only in the compositional range of Bøggild intergrowths (An_{35} to An_{66}). Calibration curves were obtained by analyzing independently well-characterized standard specimens of feldspar by both EPMA and IMA. In this way a relationship between secondary ion emission intensity and element concentration in feldspars was established. It should be noted that secondary ion intensity is a function of crystal orientation as well as concentration, such that calibration curves must be constructed for secondary ion intensity ratios. While the absolute intensities of

ions from two elements may vary, the ratios do not. Each lamella in labradorite is more than 50 nm in thickness, and the boundaries between lamellae are almost uniformly parallel to each other, at a particular composition (Miúra *et al.*, 1974, 1975). Consequently it was not necessary to use a small spot when depth profiling; in fact it was preferable to use a wide beam to minimize edge effects in the eroded crater. In peristerite and cryptoperthite lamellae, however, the thickness of one of the two lamella types is below 50 nm and the lamellar boundaries are usually irregular. It is thus necessary to use a finely-focussed ion beam to avoid overlap of the spot onto adjacent lamellae. Therefore, the compositions of peristerite and cryptoperthite lamellae can be determined mainly by using "point analysis" with a very small diameter primary ion beam in the ion microprobe analyzer (see Fig. 1).

Two-phase fields of peristerite and Bøggild intergrowths may be formed either by a two-phase binary "loop" or by solvus (Smith, 1975; Barron, 1972; Nord *et al.*, 1978). The question of whether the precursors to peristerite or Bøggild lamellae are spinodally controlled can be addressed by exploring the compositions of the two phases, because compositional fluctuations are the precursors to spinodal decomposition. The ion microprobe analyzer has the resolution to resolve such compositional fluctuations, and

¹ On leave from Department of Mineralogical Sciences and Geology, Faculty of Science, Yamaguchi University, Yamaguchi 753, Japan.

the problem can be tested on coarse (>75 nm) exsolution lamellae.

Analytical procedure

The specimens used in this study are peristerites from Ontario (precise locality unknown; shown as P-1, 2) and Hybla, Ontario (H-1, 2, 3) (*cf.* Ribbe, 1962), and cryptoperthites from Quebec, Canada (CC-1), Larvik, Norway (CND-1, 2), and Johana, Japan (CJ-1). These specimens were polished with 0.25 μm diamond paste so that the polished surface would be closely parallel to lamellar planes whose orientation had been determined by previous TEM study of surface replicas. The specimens were then analyzed by EPMA (JXA-50A) at 15kV prior to performing the IMA analysis (see Table 1). The mean bulk compositions determined by EPMA are accurate to approximately 4 mole percent of the Or content in peristerite or 0.6 percent in cryptoperthite. The Ab contents are accurate to 0.4 percent in cryptoperthite, and 0.3 percent in peristerite. A Hitachi ion microprobe analyzer, IMA-2, incorporating an electron spray gun (*cf.* Nakamura *et al.*, 1976; Miúra and Tomisaka, 1978) was used to collect the secondary ion intensities from the surfaces of these specimens. The specimens were bombarded with a positively-charged primary beam of oxygen ($^{16}\text{O}_2^+$) at 12kV, using a beam diameter of approximately 5 μm , a beam current of $5 \times 10^{-8}\text{A}$, and an electron spray gun current of 4 μA .

Secondary ion intensities of the $^{39}\text{K}^+$, $^{23}\text{Na}^+$, and $^{27}\text{Al}^+$ isotopes were used to determine the Or, Ab,

Table 1. Bulk compositions of iridescent peristerites and cryptoperthites determined by electron microprobe

	P-1	P-2	H-1	H-3	CC-1	CND-1	CND-2	CJ-1
SiO_2	67.02	66.45	67.43	67.26	64.84	64.54	64.58	66.82
Al_2O_3	20.59	21.13	20.58	20.27	22.25	21.67	21.92	20.08
K_2O	0.38	0.35	0.14	0.79	4.90	6.02	6.92	8.47
Na_2O	10.87	10.39	11.29	10.99	6.61	6.28	5.69	5.51
CaO	1.85	2.00	1.12	0.93	2.19	1.68	0.74	0.09
Total	100.71	100.32	100.56	100.24	100.79	100.19	99.85	100.97
Or(mol.%)	2.0(1)	1.9(1)	0.8(1)	4.3(1)	29.5(1)	35.4(1)	42.7(1)	50.3(2)
Ab(mol.%)	89.5(3)	88.7(3)	94.1(3)	91.4(3)	60.0(2)	56.3(2)	53.4(2)	49.3(2)
An(mol.%)	8.5(1)	9.4(1)	5.1(1)	4.3(1)	10.5(1)	8.3(1)	3.9(1)	0.4(1)

* Estimated standard deviations are in parentheses.

and An contents, because $^{27}\text{Al}^+$ has the highest relative yield of all the elements in the feldspars and because $^{27}\text{Al}^+$ and $^{23}\text{Na}^+$ are unique isobars for which interference by other ion species is very small. The Or and Ab (or An) contents in peristerite and cryptoperthite lamellae could be calculated from the ion intensity ratios K^+/Al^+ and Na^+/Al^+ , just as for the ratios in labradorite (Miúra and Tomisaka, 1978).

The measured secondary ion intensity ratio of bulk standard specimens determined with IMA can be related to the atomic ratio determined with EPMA by using correction factors f_{Or} and f_{Ab} (or f_{An}). These correlations are shown by the working curves which determine the compositions of the exsolution lamellae.

In attempting to obtain depth profiles of these materials, no regular variation in the ratios $I_{\text{K}^+}/I_{\text{Al}^+}$ and $I_{\text{Na}^+}/I_{\text{Al}^+}$ could be found as erosion proceeded through the layers. This is due in part to smaller or larger lamellae intervening between host lamellae, and also to irregular curved boundaries of the lamellar texture. The average sputtering rate was usually about 30 nm/min. Electronic aperturing, which discriminates against ions from the crater walls, was used when appropriate in raster mode. An alternative approach was made using point (5 μm diameter) analyses on a grid pattern, with grid meshes of 10, 50, and 100 μm .

The working curves for estimating Or and Ab (or An) contents of the lamellae were determined on a standard specimen, which was chosen from the specimens of each intergrowth type so as to make the measured and corrected ion intensity ratios equal; *i.e.* the values of the correction factors f_{Or} and f_{Ab} (or f_{An})

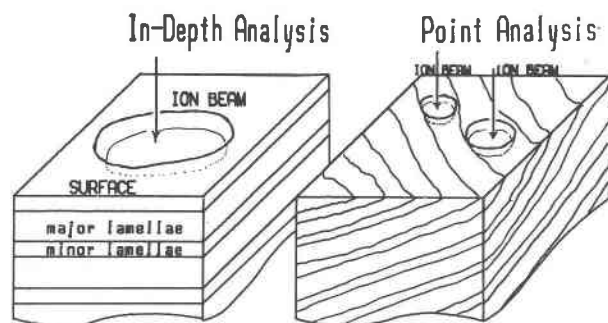


Fig. 1. Schematic diagram of in-depth and point analyses. In-depth analysis, normal to the regular parallel-sided lamellae, was used for labradorite with a beam diameter of about 50 μm . On the other hand, the point method was used for analysis of the smallest area possible, and can be used on any surface with exposed lamellar texture, such as in peristerite and cryptoperthite which have fine and non-uniform lamellar structures. Point (5 μm diameter) analyses are best made on a grid pattern, with grid meshes of 10, 50 and 100 μm .

Table 2. Observed and corrected ion intensity ratios and Or and Ab (or An) correction factors for the establishment of working curves to determine Or and Ab (or An) contents in peristerite and cryptoperthite lamellae

Specimen	Iridescence Color	$(I_{Na^+}/I_{Al^+})_{obs}$	$\frac{f_{An}}{f_{Ab}}^*$	$(I_{Na^+}/I_{Al^+})_{corr}$	$(I_{K^+}/I_{Al^+})_{obs}$	K_{100}^{**}	f_{Or}	$(I_{K^+}/I_{Al^+})_{corr}$
P-1	Blue	0.69	1.22	0.84	0.009	0.010	2.11	0.020
P-2	Whitish blue	0.64	1.27	0.81	0.008	0.009	2.13	0.018
H-1	Orange-red	0.81	1.11	0.90	0.003	0.003	2.33	0.008
H-3	Whitish blue	0.92	1.00	0.92	0.038	0.041	1.00	0.041
CC-1	Whitish blue	0.54	0.90	0.49	0.29	0.31	1.02	0.32
CND-1	Whitish blue	0.48	0.95	0.46	0.38	0.41	1.01	0.41
CND-2	Whitish blue	0.44	1.00	0.44	0.46	0.49	1.00	0.49
CJ-1	Whitish blue	0.39	1.05	0.41	0.55	0.59	0.99	0.58

* For cryptoperthite the factor is f_{Ab} .

** $K_{100} = 1.074 \times (I_{K^+}/I_{Al^+})_{obs}$ to correct for natural isotopic abundance.

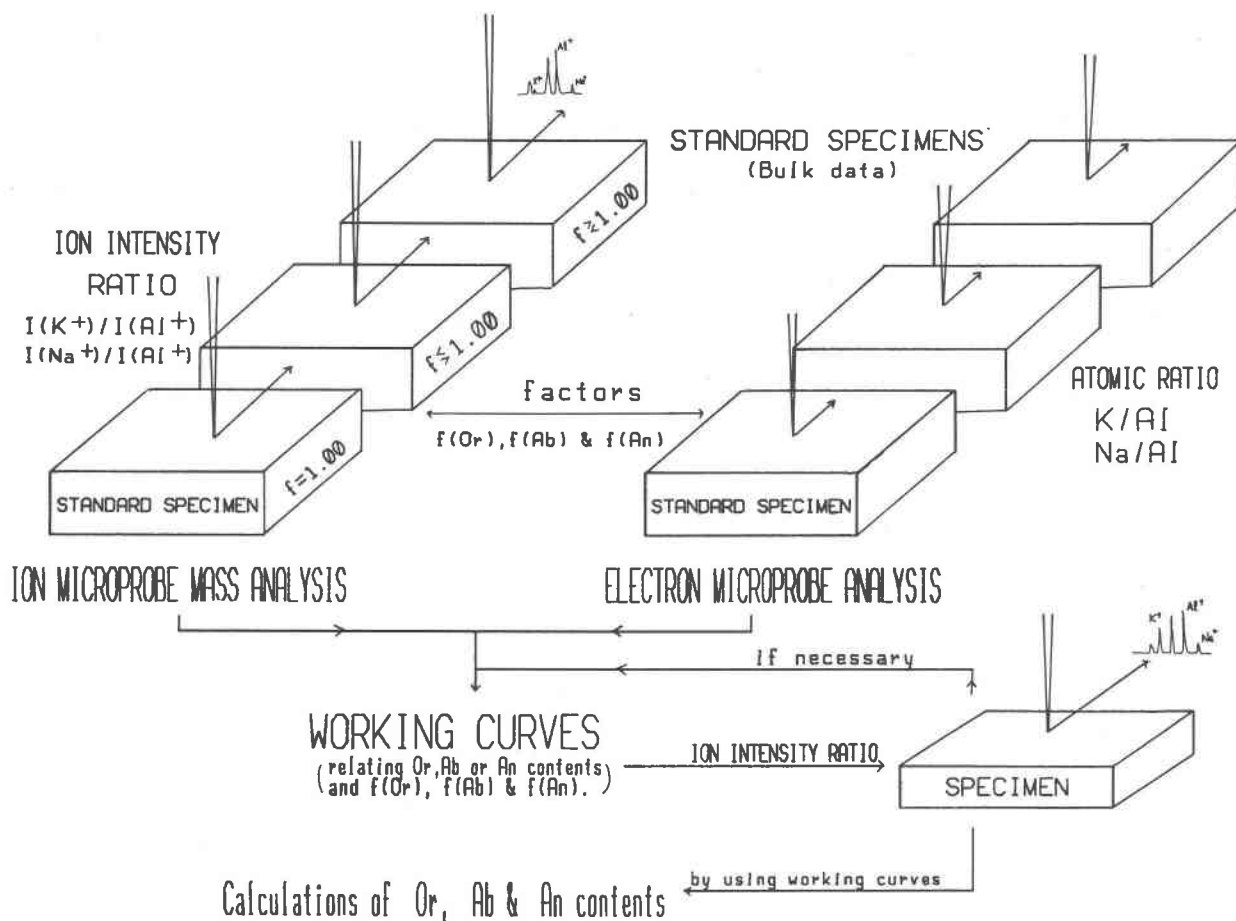


Fig. 2. Schematic procedure of quantitative ion microprobe analysis of exsolution lamellae in this study.

were arranged to equal unity in one of the standard specimens, as listed in Table 2.

The compositions of the exsolution lamellae were determined from the working curves based on measured ion intensity ratios. These ratios sometimes included data from adjacent lamellae, or inclusions, or both. The ion intensity ratios, therefore, had to be screened from the raw data. The analytical procedure of the quantitative IMA analysis is shown in Figure 2.

Working curves for determining Or and Ab (or An) contents

The correction factors f_{Or} and f_{Ab} for cryptoperthite, and f_{An} for peristerite, which are dependent on the average atomic fraction of Al, are determined from the ratios of the corrected and measured ion intensity ratios $(I_{K^+}/I_{Al^{3+}})_{corr}/1.074(I_{K^+}/I_{Al^{3+}})_{obs}$ and $(I_{Na^+}/I_{Al^{3+}})_{corr}/(I_{Na^+}/I_{Al^{3+}})_{obs}$, respectively. These values are listed in Table 2 and plotted against the known bulk Or and Ab (or An) contents in Figures 3 and 4, where Ab (mole percent) = 100 - An - Or in each intergrowth. The equations for the regression lines relating $(I_{K^+}/I_{Al^{3+}})_{corr}$ and $(I_{Na^+}/I_{Al^{3+}})_{corr}$ to Or and Ab (or An) contents, respectively, are given in Tables 3 and 4.

The working curves for estimating the Or and Ab (or An) contents of cryptoperthite and peristerite la-

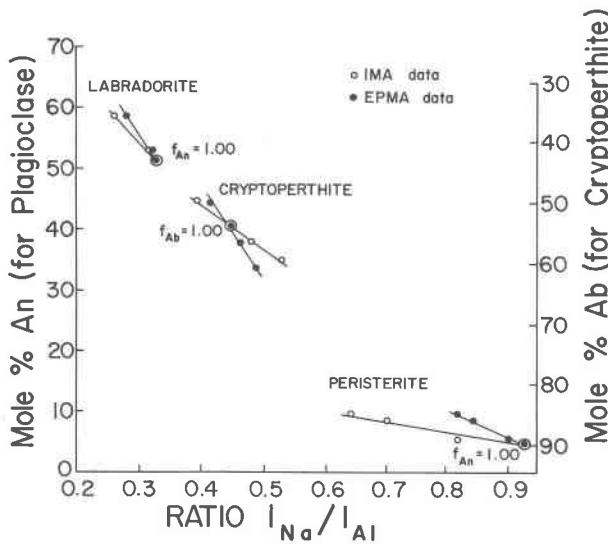


Fig. 3. Working curves for mole percent An (in plagioclase) or Ab (in cryptoperthite). Ab(mol.%) = 100 - An - Or. Ratios I_{Na^+}/I_{Al} in standard specimens are obtained from EPMA data (cf. Table 1) which are shown by filled circles, and from IMA data (cf. Table 2) shown by open circles. The values of the correction factors f_{An} (or f_{Ab}) were arranged to equal unity in one of the standard specimens.

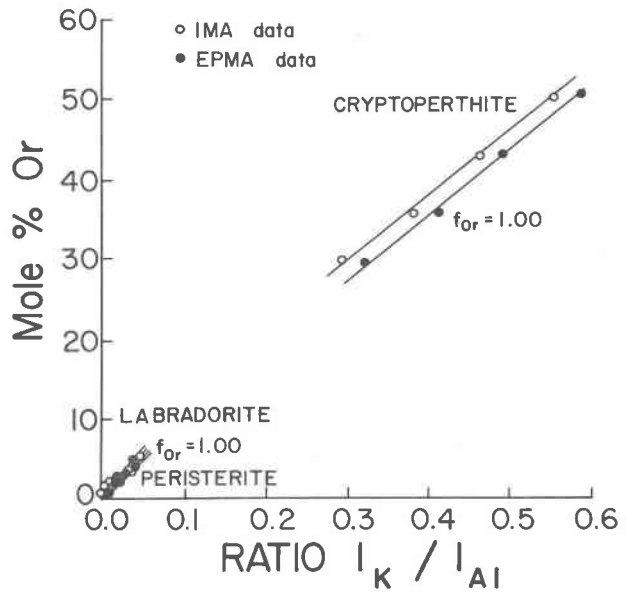


Fig. 4. Working curve for mole percent Or in iridescent feldspars. The observed ion intensity ratios shown by open circles are those uncorrected for natural isotopic abundance.

mellae show good correlations between the values of Or and Ab (or An) contents as determined by EPMA and the normalized $^{39}K^+$ and $^{23}Na^+$ intensities as measured on standards with the IMA. Thus the composition of exsolution lamellae can be determined from the working curves listed in Table 3.

The results of spot analyses of cryptoperthites and peristerites are plotted in Figure 5 and listed in Ta-

Table 3. Equations for regression lines relating the observed and corrected ion intensity ratios to An and Or contents in peristerite lamellae

Equation for least-squares regression line	Correlation coefficient
$An(mol.\%) = 49.4 - 49.1(I_{Na^+}/I_{Al^{3+}})_{corr}$ (6.1) * (6.6)	-0.99
$f_{An} = 1.87 - 0.94(I_{Na^+}/I_{Al^{3+}})_{obs}$ (0.02) (0.02)	-0.99
$Or(mol.\%) = -0.06 + 106.0(I_{K^+}/I_{Al^{3+}})_{corr}$ (0.22) (8.4)	0.99
$f_{Or} = 2.49 - 39.7(I_{K^+}/I_{Al^{3+}})_{obs}$ (0.03) (2.8)	-0.99

*The numbers in parentheses below the regression coefficients are estimated standard deviations.

Table 4. Equations for regression lines relating the observed and corrected ion intensity ratios to Or and Ab contents in cryptoperthite lamellae

Equation for least-square regression line	Correlation coefficient
Or(mol.%) = $3.0 + 81.0(I_{K^+}/I_{Al^+})_{corr}$ (4.3) * (7.2)	0.99
$f_{Or} = 1.1 - 0.12(I_{K^+}/I_{Al^+})_{obs}$ (0.0) (0.03)	-0.99
Ab(mol.%) = $0.82 + 119.2(I_{Na^+}/I_{Al^+})_{corr}$ (3.5) (4.7)	0.99
$f_{Ab} = 1.33 - 0.75(I_{Na^+}/I_{Al^+})_{obs}$ (0.8) (1.5)	-0.99

*The numbers in parentheses below the regression coefficients are estimated standard deviations.

bles 5 and 6. The calculated bulk Or and Ab (or An) contents were obtained as follows:

$$C_{calc} = (C_A N_A + C_B N_B) / (N_A + N_B) \quad (1)$$

where N_A and N_B are numbers of minor and major lamellae measured, and C is Or or Ab (or An) content. Equation 1 can be rewritten as

$$C_{calc} = [C_A(N_A/N_B) + C_B] / [1 + (N_A/N_B)] \quad (2)$$

where the ratio N_A/N_B is replaced by the lamellar thickness ratio which is obtained from electron mi-

Table 5. Results of point analysis in iridescent peristerites from Hybla. The estimated standard deviations are given in parentheses

Specimen	Major lamellae			Minor lamellae		
	An(mol.%)	Or(mol.%)	No. of points	An(mol.%)	Or(mol.%)	No. of points
H-1	2.4(1.9)	1.2(1.2)	8	18.7(1.5)	0.8(0.4)	15
H-2*	2.5(1.9)	1.1(1.1)	8	23.0(1.7)	2.9(2.0)	7
Mean	2.4(1.9)	1.2(1.2)		20.9(1.6)	1.9(1.0)	

* The composition of H-2 peristerite is $An_{7.0}Or_{0.9}$.

crographs. The values for this parameter are 3.96 (in H-1), 4.23 (in H-2), 2.00 (in CC-1), and 1.23 (in CJ-1).

The bulk Or and Ab (or An) contents calculated from the IMA data are within 6 or 14 percent of the An content as determined by EPMA for H-1 and H-2 peristerites, respectively; and within 8 or 3 percent in Or content and 1 or 9 percent in Ab content of CC-1 and CJ-1 cryptoperthites, respectively (Table 7).

Discussion

IMA analysis problem

The secondary ion mass spectrum of feldspar is complicated (see Meyer *et al.*, 1974; Shimizu *et al.*, 1978), due to mass overlapping of various ion species at the same nominal mass numbers. The $^{27}Al^+$ and $^{23}Na^+$ signals used in this study should be free from overlaps, but Ca and Si ions are overlapped by several complex molecular ions. While there may be minor interference with $^{39}K^+$, we assumed this to be small or constant, and the consistency of the results vindicates this assumption. Hence only Al, Na, and K ions were used to determine the feldspar compositions.

The distribution of lamellae on the analysis surface can be determined by taking an electron micrograph of replicas of the side faces of a cube-shaped specimen. Depth-profiling ion microprobe analysis of the slightly irregular lamellae of the cryptoperthites

Table 6. Results of point analysis in pale-blue iridescent cryptoperthites from Quebec and Johana. The estimated standard deviations are given in parentheses

Specimen	Major lamellae			Minor lamellae		
	Or(mol.%)	Ab(mol.%)	No. of points	Or(Mol.%)	Ab(mol.%)	No. of points
CC-1	10.3(0.7)	58.8(1.0)	13	46.7(1.3)	53.3(2.4)	3
CJ-1	33.7(2.5)	56.1(2.5)	22	66.4(7.2)	36.5(3.0)	3

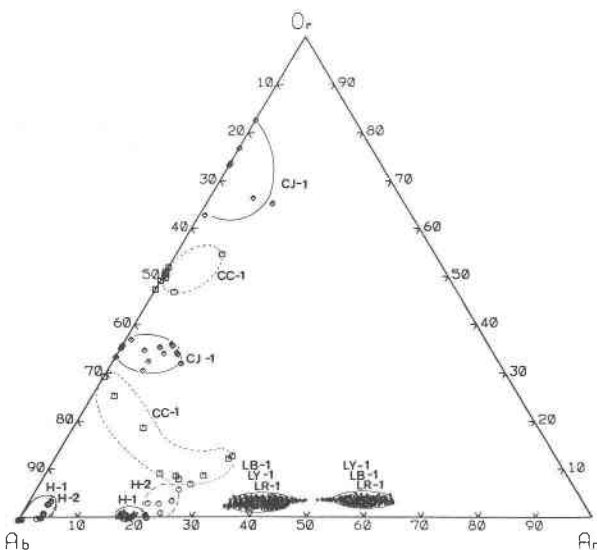


Fig. 5. Results of point analysis of two kinds of lamellae in peristerite and cryptoperthite, together with those in labradorite.

Table 7. Calculated bulk compositions from IMA data in Tables 5 and 6, compared with the bulk compositions determined by EPMA listed in Table 1. Equation (2) is used to obtain this comparison between IMA and EPMA data

Specimen	I M A data			E M data Lamellar thickness(nm)	E P M A data			C a l c u l a t e d data		
	Or	Ab	An(mol.%)		Or	Ab	An(mol.%)	Or	Ab	An(mol.%)
H-1	1(1)	97(2)	2(2)	103	0.8	94.1	5.1	1.0	93.6	5.4
	1(1)	80(2)	19(2)*	26						
H-2	1(1)	97(2)	2(2)	131	0.9	92.1	7.0	1.4	92.6	6.0
	3(2)	74(2)	23(2)	31						
CC-1	15(8)	66(5)	19(6)	76	29.5	60.0	10.5	27.0	60.0	12.7
	51(3)	49(6)	0(0)	38						
CJ-1	35(2)	59(7)	6(4)	74	50.3	49.3	0.4	51.6	45.1	3.3
	72(7)	28(5)	0(0)	60						

* Another composition of two lamellae in IMA data is listed below. The estimated standard deviations in IMA data are given in parentheses.

and peristerites may give an irregularly varying signal, while for the regular lamellae of labradorites a regularly varying signal, which oscillates between two extremes, is obtained. In the latter case the compositions of the two lamellar phases are thus easily measured, and the thicknesses correlated with the electron micrograph data (see Miúra and Tomisaka, 1978). In the point analysis approach on the less regular lamellae, there are many data points which reflect overlap of the ion beam on to more than one lamella, or the presence of inclusions. If a large number of measurements is taken at many points, usually selected on a grid pattern, those data showing the extreme compositional values can be selected as being representative of the lamellae, and the remainder discarded.

Compositions of exsolution lamellae

The working curve method for determining feldspar compositions by ion probe is a valuable and reliable technique providing certain precautions are observed. Firstly, there must be at least three similar 'standard' specimens to establish a linear regression line. Secondly, discontinuities may be expected across a solid-solution series (Steele *et al.*, 1977), which may arise because of varying complex microstructure, structural state, or the presence of inclusions (*cf.* Miúra, 1978a). For this reason the working curves must not be extrapolated beyond the range of the standards used.

The bulk compositions as determined by ion probe

(calculated from lamellae data) and electron probe (measured directly) deserve some comment. For specimen H-1 the results agree within the limit of error. For H-2 there is a difference of 1 percent An absolute at a level of 6 percent An, implying perhaps that complete resolution of the two phases was not achieved with the ion probe. This could possibly be due to the presence of smaller lamellae about 30 nm in thickness, or markedly irregular lamellar boundaries (see Miúra, 1978b). A further small error may arise if there are substitutions such as Fe³⁺ for Al, or if there are vacancies in the alkali site, but no attempt has been made to allow for this.

Orthoclase contents in cryptoperthites CC-1 and CJ-1 show deviations of 2.5 and 1.3 percent absolute, respectively, when compared with those from EPMA, and the An contents show larger deviations. This may be partly because of the rapid change of the relative lamellar thicknesses in a small region, and partly because of incomplete resolution where the smaller thickness is less than 60 to 70 nm (see Miúra, 1978c). Nevertheless, the IMA analyses give sufficiently good agreement that the results may be considered valid.

The data in Table 7 are consistent with the composition of the lamellar pairs being different by at least 17 percent An in H-1 and 21 percent An in H-2. The difference in Or content, however, is at most 1 mole percent in H-1 but greater in H-2, which may be richer in minor lamellae. However, the Or standard deviations do not appear to be related to lamellar

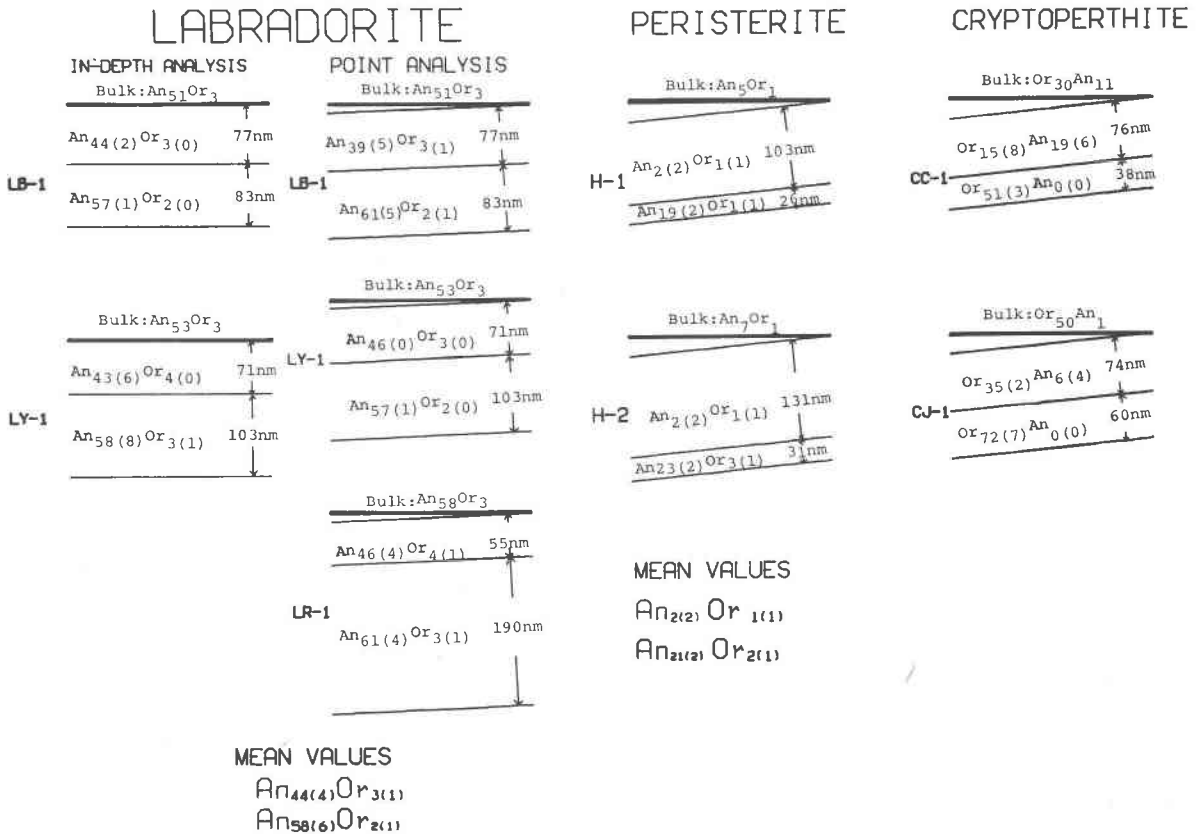


Fig. 6. Schematic diagram of IMA analytical results together with lamellar thicknesses. Bulk compositions for each specimen are shown on the upper surfaces. Labradorite from a previous study (Miúra and Tomisaka, 1978) is shown for comparison. The lamellar compositions of the labradorite examples change as a function of bulk composition, rather than from thickness variation in lamellae of constant compositions. The same phenomenon can be seen for peristerite and cryptoperthite. The angle between surface and lamellar boundaries in point analysis is exaggerated.

composition. These data are close to the results of Cliff *et al.* (1975) obtained from electron microscopy, and of McLaren (1974). The results in this study show that the peristerite region ranges from $An_{2\pm 2}$ to $An_{21\pm 2}$.

Ion probe analysis of fine feldspar lamellae has the advantage over other methods used previously, in that data for all three components are obtained. This permits examination of the Or content of plagioclase lamellae, and this study has shown that peristerite lamellae vary slightly in this respect. Similarly, Bøggild lamellae show variations in Or at the one sigma level (Miúra, 1977; Miúra and Tomisaka, 1978). Rather than speculate on the precise meaning of these observations, we will merely point out that future discussions on the mechanisms by which plagioclase exsolution take place should take account of this third component.

In CC-1 the difference in composition (Δ) of the la-

mellae are ΔOr_{36} and ΔAn_{19} , and for CJ-1 ΔOr_{37} and ΔAn_6 . Cryptoperthite lamellae compositions have been reported by Brown *et al.* (1974) and by Sipling and Yund (1976), but their data did not include the third An component. Figure 5 shows that this third component is in fact important, particularly in specimen CC-1 where the extension into the ternary system is large. This specimen should perhaps be more correctly assigned the name 'cryptoantiperthite.'

Acknowledgments

We thank Mr. I. Nakamura of the Central Research Laboratory, Hitachi Ltd., for facilities and collaborating in the IMA study, and Professor I. Sunagawa of Tohoku University for his interest in this study. We are also grateful to Drs. D. Stewart and G. Nord, Jr. of the U.S. Geological Survey, Professor R. Yund and Dr. Tullis of Brown University, and Dr. C. Meyer, Jr. of NASA, Houston for discussion. Professors C. Klein and A. E. Bence are thanked for critically reviewing the manuscript. An operating grant (A3549) from the National Sciences and Engineering Research Council of Canada assisted in this work.

References

- Barron, L. M. (1972) Thermodynamic multicomponent silicate equilibrium phase calculations. *Am. Mineral.*, 57, 809–823.
- Brown, W. L., M. Grandais, J. T. Iiyama, J. Roux and C. Willaime (1974) A study of exsolution in synthetic alkali feldspar. *Proc. Eighth Int. Cong. Electron Microscopy, Canberra, 1*, 506–507.
- Cliff, G., P. E. Champness, H.-U. Nissen and G. W. Lorimer (1975) Analytical electron microscopy of exsolution lamellae. In H.-R. Wenk, Ed., *Electron Microscopy in Mineralogy*, p. 258–265. Springer-Verlag, Berlin.
- McLaren, A. C. (1974) Transmission electron microscopy of the feldspars. In W. S. MacKenzie and J. Zussman, Eds., *The Feldspars*, p. 378–424. Manchester Press, Manchester, England.
- Meyer, C. Jr., D. H. Anderson and J. G. Bradley (1974) Ion microprobe mass analysis of plagioclase from 'non-mare' lunar sample. *Proc. Fifth Lunar Sci. Conf., Geochim. Cosmochim. Acta Suppl. 5*, 685–708.
- MiÛra, Y. (1977) Labradorescence-1-. *J. Gemmol. Soc. Japan*, 4(4), 3–11.
- (1978a) Color zoning in labradorescence. *Mineral J.*, 9(2), 91–105.
- (1978b) Iridescence in peristerite (Peristerism). *J. Gemmol. Soc. Japan*, 5(2), 3–12.
- (1978c) Iridescence in alkali feldspar. *J. Gemmol. Soc. Japan*, 5(3), 15–25.
- and T. Tomisaka (1978) Ion microprobe mass analysis of exsolution lamellae in labradorite feldspar. *Am. Mineral.*, 53, 584–590.
- , ——— and T. Kato (1974) Experimental and theoretical approaches to iridescent labradorite. *Mem. Geol. Soc. Japan*, 11, 145–165.
- , ——— and ——— (1975) Labradorescence and the ideal behavior of thicknesses of alternate lamellae in the Bøggild intergrowth. *Mineral. J.*, 7, 526–541.
- Nakamura, I., Y. Hirahara, A. Shibata and T. Tamura (1976) Surface analysis of insulating materials by means of an ion microprobe analyzer. *Mass Spectroscopy*, 24(2), 163–172.
- Nord, G. L., Jr., J. Hammarstrom and E-an Zen (1978) Zoned plagioclase and peristerite formation in phyllites from southwestern Massachusetts. *Am. Mineral.*, 63, 947–955.
- Ribbe, P. H. (1962) Observations on the nature of unmixing in peristerite plagioclase. *Norsk Geol. Tidsskr.*, 42(2), 138–151.
- Shimizu, N., M. P. Semet and C. J. Allègre (1978) Geochemical applications of quantitative ion-microprobe analysis. *Geochim. Cosmochim. Acta*, 42, 1321–1334.
- Sipling, P. J. and R. A. Yund (1976) Experimental determination of the coherent solvus for sanidine-high albite. *Am. Mineral.*, 61, 897–906.
- Smith, J. V. (1975) Phase equilibria of plagioclase. In P. H. Ribbe, Ed., *Feldspar Mineralogy*. Mineral. Soc. Am. Short Course Notes 2.
- Steele, I. M., I. D. Hutcheon, T. N. Solberg, R. N. Clayton and J. V. Smith (1977) Ion microprobe analysis of plagioclase feldspars ($\text{Ca}_x\text{Na}_{1-x}\text{Al}_{1+x}\text{Si}_{3-x}\text{O}_8$) for major and minor elements. *Eighth Int. Conf. X-ray Optics and Microanalysis and Twelfth Annual Conf. Microbeam Analysis Soc., Boston*, 180A–F.

Manuscript received, February 16, 1979;
accepted for publication, June 29, 1979.